Vol 17 No 10, October 2008
1674-1056/2008/17(10)/3867-08

Chinese Physics B

© 2008 Chin. Phys. Soc.
and IOP Publishing Ltd

First-principles calculations for electronic, optical and thermodynamic properties of ZnS*

Hu Cui-E(胡翠娥)[a], Zeng Zhao-Yi(曾召益)[a], Cheng Yan(程 艳)[a], Chen Xiang-Rong(陈向荣)[a)b)†], and Cai Ling-Cang(蔡灵仓)[c]

[a] *School of Physical Science and Technology, Sichuan University, Chengdu* 610064, *China*
[b] *International Centre for Materials Physics, Chinese Academy of Sciences, Shenyang* 110016, *China*
[c] *Laboratory for Shock Wave and Detonation Physics Research, Institute of Fluid Physics, Chinese Academy of Engineering Physics, Mianyang* 621900, *China*

(Received 22 January 2008; revised manuscript received 30 May 2008)

The electronic, optical and thermodynamic properties of ZnS in the zinc-blende (ZB) and wurtzite (WZ) structures are investigated by using the plane-wave pseudopotential density functional theory (DFT). The results obtained are consistent with other theoretical results and the available experimental data. When the pressures are above 20.5 and 27 GPa, the ZB-ZnS and the WZ-ZnS are converted into indirect gap semiconductors, respectively. The critical point structure of the frequency-dependent complex dielectric function is investigated and analysed to identify the optical transitions. Moreover, the values of heat capacity C_V and Debye temperature Θ at different pressures and different temperatures are also obtained successfully.

Keywords: density functional theory, electronic structure, optical property, thermodynamics property

PACC: 7115M, 7125T, 7800, 6740K

1. Introduction

Recently, research on Zn–VI based compound semiconductors has gained considerable attention due to their potential applications in the short-wavelength light-emitting devices. Because of their high polarities and large excitonic binding energies, Zn-based semiconductors are of great interest not only in practical applications but also in fundamental science.[1,2] Under an ambient pressure, there are two types of structures in Zinc Sulfide (ZnS), i.e. the high temperature phase hexagonal wurtzite (WZ) structure and the low temperature phase cubic zinc-blende (ZB) structure. [3] Nanoscience and nanomaterials carve out a way for scientists to develop the unusual materials for industrial applications. Through the technique of phase controlled synthesis, nanoscale ZnS solids in both ZB and WZ phases were successfully prepared.[4] Fundamentally, the WZ-ZnS presents a different electronic structure from the ZB-ZnS. The band gaps of the ZB-ZnS and the WZ-ZnS are 3.70 and 3.91 eV, respectively.[5] Furthermore, Geng *et al*[6] found that the ZB-ZnS and the WZ-ZnS had wide band gaps of 3.5–3.7 and 3.7–3.8 eV, respectively, when they synthesized ZnS nanowires via a thermal evaporation method.

In addition, Bellotti *et al*[7] found that the WZ-ZnS was more suitable for fabricating the electroluminescent devices because it exhibited a higher ionization transition rate and therefore had a higher optical gain. Even though a series of studies was devoted to clarifying the optical properties of the WZ-ZnS early in the 1970s, their results always led one to fall into confusion due to the mixture of the WZ and the ZB phases.[8,9] To design the semiconductor devices appropriately, basic researches on the fundamental physical properties, such as the electronic, optical and thermodynamic properties, are needed. Thus, in this work, we will make an investigation on the electronic, optical and thermodynamic properties of ZnS in both ZB and WB structures by using first-principles calculations. In Section 2, we give a brief description of the theoretical computational method. The results of structural, thermodynamic and electronic properties are presented and analysed in Section 3. Conclusion is drawn in the last Section.

*Project supported by the National Natural Science Foundation of China (Grant No 10776022), the State Key Program of National Natural Science of China (Grant No 60436010), and the Fund of Key Laboratory for Shockwave and Detonation Physics (Grant No 9140C6711010805).

†Corresponding author. E-mail: xrchen@126.com

2. Theoretical method

In our calculations, the electronic wave functions are expanded in a plane-wave basis set with an energy cut-off of 500.00 eV. Pseudo-atomic calculations are performed for Zn $3p^6 3d^{10} 4s^2$ and S $3s^2 3p^4$. As for the Brillouin-zone k-point sampling, 10×10×6 and 10×10×10 Monkhorst-Pack meshes[10] are employed for the WZ-ZnS and the ZB-ZnS, respectively, where the self-consistent convergence of the total energy is at 10^{-6} eV/Atom. The plane-wave pseudopotential density functional theory (DFT) method is applied, together with the generalized gradient approximation (GGA)[11] for exchange-correlation functional in the scheme of Perdew–Wang (PW)[12] formula. All the calculations are implemented through the Cambridge Serial Total Energy Package (CASTEP) scheme.[13]

To account for the finite temperature properties of a crystal, we here apply the quasi-harmonic Debye model,[14] in which the non-equilibrium Gibbs functionG^* $(x; P, T)$ can be written as

$$G^*(x; P, T) = E(x) + PV(x) + A_{\mathrm{Vib}}(x; T), \qquad (1)$$

where $E(x)$ is the total energy of the crystal, which can be determined from the electronic structure calculations. The term PV corresponds to the constant hydrostatic pressure condition. The term, A_{vib}, is the vibrational Helmholtz free energy, including both the vibrational contribution to the internal energy and the $-TS$ constant temperature condition term. It is customary to introduce the quasi-harmonic approximation[15]

$$A_{\mathrm{Vib}}(x; T) = \int_0^\infty \left[\frac{1}{2}\hbar\omega + kT \ln\left(1 - \mathrm{e}^{-\hbar\omega/kT}\right)\right] \times g(x; \omega)\mathrm{d}\omega, \qquad (2)$$

where $g(x; \omega)$ is the phonon or vibrational density of states (DOS). Using this model, we can obtain the Debye temperature Θ and the heat capacity C_V. The detailed descriptions were shown in our previous work.[16–18]

3. Results and discussion

3.1. Electronic structures

The calculated equilibrium lattice constant a for the ZB-ZnS is 5.440 Å (1Å=0.1 nm), and the lattice parameters a and c for the WZ-ZnS are 3.840 and 6.267 Å, respectively. Compared with the experimental data 5.413 Å for the ZB-ZnS,[19] 3.822 Å and 6.260 Å for the WZ-ZnS,[20] our lattice parameters are overestimated slightly (about 0.50% higher for the ZB-ZnS and 0.47% higher for the WZ-ZnS), but they are satisfactory.

The calculated band structures and total densities of state (DOSs) for the ZB-ZnS and the WZ-ZnS at P=0 GPa and T=0 K are illustrated in Fig.1. In the ZB and the WZ structures of ZnS, the valence band maximum (VBM) and conduction band minimum (CBM) occur at the Γ point. The ZB-ZnS and the WZ-ZnS have direct gaps ($\Gamma_{\mathrm{c}} - \Gamma_{\mathrm{v}}$) of 2.08 eV and 2.19 eV, respectively, which are consistent with other theoretical values 1.81 eV,[21] 2.16 eV,[22] 2.30 eV[23] for the ZB-ZnS, and 2.06 eV[24] for the WZ-ZnS, while they are smaller than the experimental data 3.7 eV [5] and 3.5–3.7 eV [6] for the ZB-ZnS, 3.91 eV [5] and 3.7–3.8 eV[6] for the WZ-ZnS. The underestimation of the band gaps is mainly due to the simple form of GGA. It is important to note that the density functional formalism is limited in its validity[25] and the band

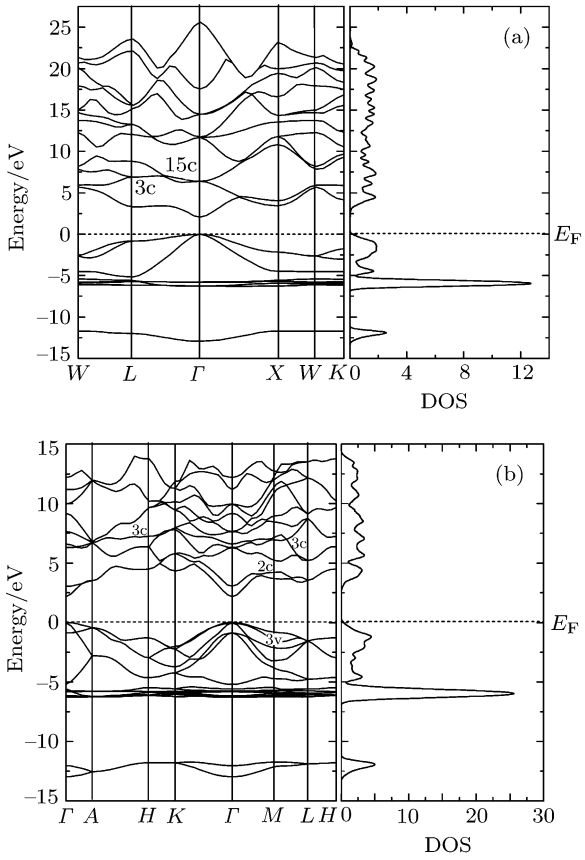


Fig.1. Band structures and densities of state (DOSs) of ZnS, where panel (a) is for the ZB structure, panel (b) is for the WZ structure, and the letters c and v represent conduction bands and valence bands, respectively.

structure derived from it cannot be used directly for comparison with experiment. Despite of the shortcoming of the GGA, the pressure derivatives can be calculated accurately in GGA and do not depend on the type or functional form of the exchange-correlation potential.[26]

In this work, we have also investigated the effect of the pressure on the energy band gaps of ZnS. To achieve this, we have calculated the values of direct and indirect gaps (E_g) at different values of pressure P. By fitting the $E_g - P$ curves to the second polynomials, we have obtained the linear and quadratic pressure-coefficients, which are listed in Table 1. For the ZB-ZnS, we can see that the direct energy gaps show an increase with pressure. The negative linear pressure coefficients indicate that the indirect band gap ($X_c - \Gamma_v$) decreases with pressure increasing. Our linear pressure coefficients are relatively close to those given by Khenata *et al*[22] through using the full-potential linear augmented plane-wave method and the local orbital (FP-LAPW+lo) method. Similarly, the indirect band gaps ($M_c - \Gamma_v$) and ($K_c - \Gamma_v$) also decrease with pressure increasing for the WZ-ZnS. The change in direct energy gap is opposite to that in indirect band gap for the WZ-ZnS. It is found from Fig.2(a) that the cross point between the direct gap ($\Gamma_c - \Gamma_v$) and the indirect gap ($X_c - \Gamma_v$) curves occurs at 20.5 GPa for the ZB-ZnS, indicating that when P >20.5 GPa, the ZB-ZnS becomes an indirect band gap semiconductor. The cross point for the WZ-ZnS occurs at 27.0 GPa shown in Fig.2(b), a little larger than that for the ZB-ZnS.

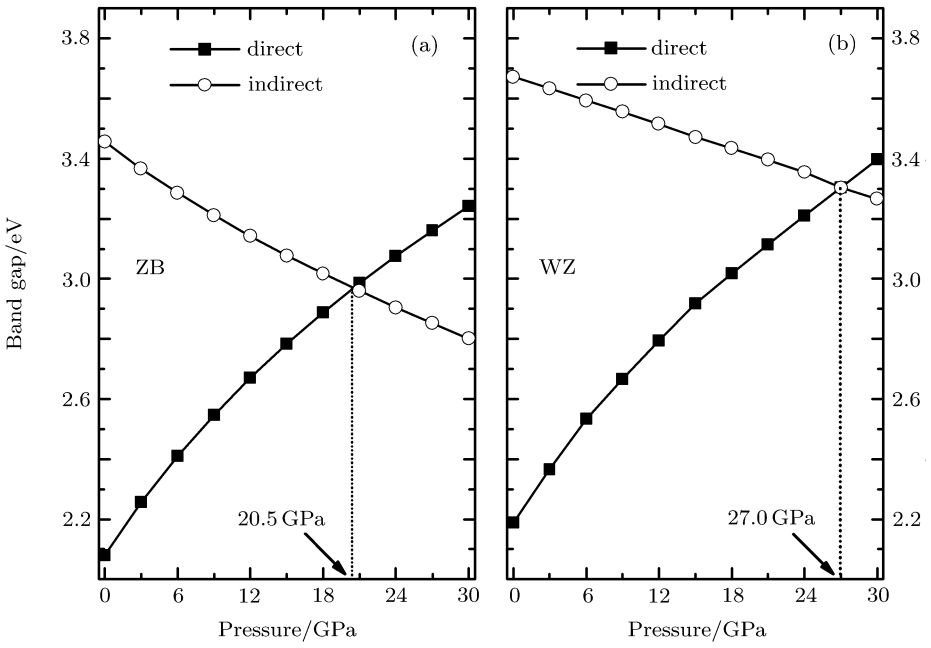


Fig.2. Direct and indirect band gaps versus pressure, where panel (a) is for Direct gap ($\Gamma_c - \Gamma_v$) and indirect gap ($X_c - \Gamma_v$) for the ZB- ZnS and panel (b) is for Direct band gap ($\Gamma_c - \Gamma_v$) and indirect band gap ($M_c - \Gamma_v$) for the WZ-ZnS.

Table 1. The band gaps for the ZB and the WZ structures of ZnS. $E_g = E_0 + aP + bP^2$, where a is in eV 10^{-2} GPa^{-1}, and b is in eV 10^{-4} GPa^{-2}. The pressure is in a range of 0–30 GPa.

	$\Gamma_c - \Gamma_v$			$X_c - X_v$			$L_c - L_v$			$X_c - \Gamma_v$			$L_c - \Gamma_v$		
ZB-ZnS	E_0	a	b	E_0	a	b	E_0	a	b	E_0	a	b	E_0	a	b
	2.08	5.43	–5.45	5.65	1.68	–1.42	4.25	4.12	–4.55	3.46	–2.84	2.29	3.28	2.31	–3.11
Ref.[22]	2.16	5.19	–9.18	5.58	1.60	–1.14	4.11	2.71	–1.22	3.01	–1.6	2.34	3.16	1.59	–3.25
	$\Gamma_c - \Gamma_v$			$M_c - M_v$			$K_c - K_v$			$M_c - \Gamma_v$			$K_c - \Gamma_v$		
WZ-ZnS	E_0	a	b	E_0	a	b	E_0	a	b	E_0	a	b	E_0	a	b
	2.19	5.52	–5.33	4.51	0.85	–2.55	6.34	0.40	–1.00	3.67	–1.26	–0.32	4.39	–4.42	–4.20

In Fig.3, we show the partial densities of state (PDOSs) for the ZB and the WZ structures of ZnS at 0 GPa. Combining with total DOS in Fig.1, it is further observed that the first structure in total DOS is small but relatively protuberant at around –11.87 and –11.90 eV for the ZB-ZnS and the WZ-ZnS. The structures arise almost from the S 3s states and correspond to the lowest lying band (in Fig.1). The next structure is situated at about –5.87 and –5.95 eV below the zero energy for ZnS. They consist predominantly of Zn 3d states with a little contribution of S 3p states. From the band structures, the structures correspond to the flat bands clustered at around –6.0 eV. The structure humps between –5.30 and 0 eV in these compounds which form the upper valence band corresponding to the S 3p states partially mixed with Zn 4s states in both of the two structures. Above the Fermi level, the feature in the total DOS originates mainly from the Zn 4s and 3p states partially mixed with little of S 3p states.

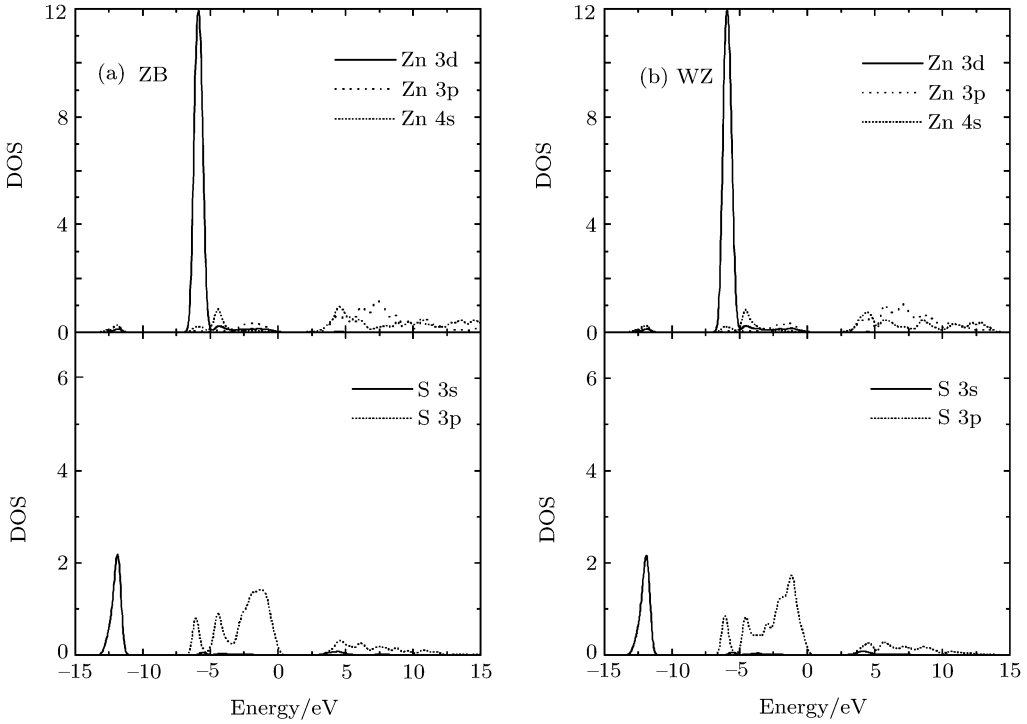


Fig.3. Partial densities of state of ZnS, where panel (a) is for the ZB structure and panel (b) is for the WZ structure.

3.2. Optical properties

The optical properties of a solid are usually described in terms of the complex dielectric function $\varepsilon(\omega) = \varepsilon_1(\omega) + \mathrm{i}\varepsilon_2(\omega)$. The imaginary part of the dielectric function $\varepsilon_2(\omega)$ in the long wavelength limit is obtained directly from the electronic structure calculation by jointly using the DOS and the optical matrix elements. The real part of the dielectric function $\varepsilon_1(\omega)$ can be derived from the imaginary part by using the Kramers–Kronig relationship. The knowledge of both the real and the imaginary parts of the dielectric function allows the calculation of important optical functions.

In Fig.4, we display the dielectric function $\varepsilon(\omega)$ for the ZB and the WZ structures of ZnS at zero pressure for a radiation up to 25 eV. For the ZB-ZnS, the imaginary part of the dielectric function includes only one component: $\varepsilon_2(\omega)$=$\varepsilon_{2x}(\omega)$=$\varepsilon_{2y}(\omega)$= $\varepsilon_{2z}(\omega)$. While, for the WZ-ZnS, the imaginary part of the dielectric function are resolved into two components: $\varepsilon_{2xy}(\omega)$=$\varepsilon_{2x}(\omega)$=$\varepsilon_{2y}(\omega)$ (the average of the spectra for polarizations along the x and y directions) and $\varepsilon_{2z}(\omega)$ (the polarization vector being parallel to the z direction). The averaged function $\varepsilon_2(\omega)$=$(\varepsilon_{2x}+\varepsilon_{2y}+\varepsilon_{2z})/3$ is also included. The analysis of the $\varepsilon_2(\omega)$ curves shows that the first critical points of the dielectric function occur at 2.08 and 2.19 eV for the ZB-ZnS and the WZ-ZnS respectively. These points are $\Gamma_{\mathrm{v}} - \Gamma_{\mathrm{c}}$ splitting, giving the thresholds for direct optical tran-

sitions. This is known as the fundamental absorption edge. These critical points are followed by many prominent peaks. For the ZB-ZnS, the three peaks at about 4.31, 5.89 and 7.75 eV are presented mainly due to the interband transitions from Γ_{15c} to Γ_c, K_c to K_v and L_{3c} to L_v, respectively. For the WZ-ZnS, the prominent peaks are at about 3.41, 5.56 and 6.77 eV, corresponding to the transitions from K_{3c} to K_c, M_{2c} to M_{3v} and L_{3c} to L_v, respectively. Meanwhile, a peak in imaginary part $\varepsilon_2(\omega)$ does not correspond to a single interband transition, for many direct or indirect transitions can be found in the band structure with an energy corresponding to the same peak.

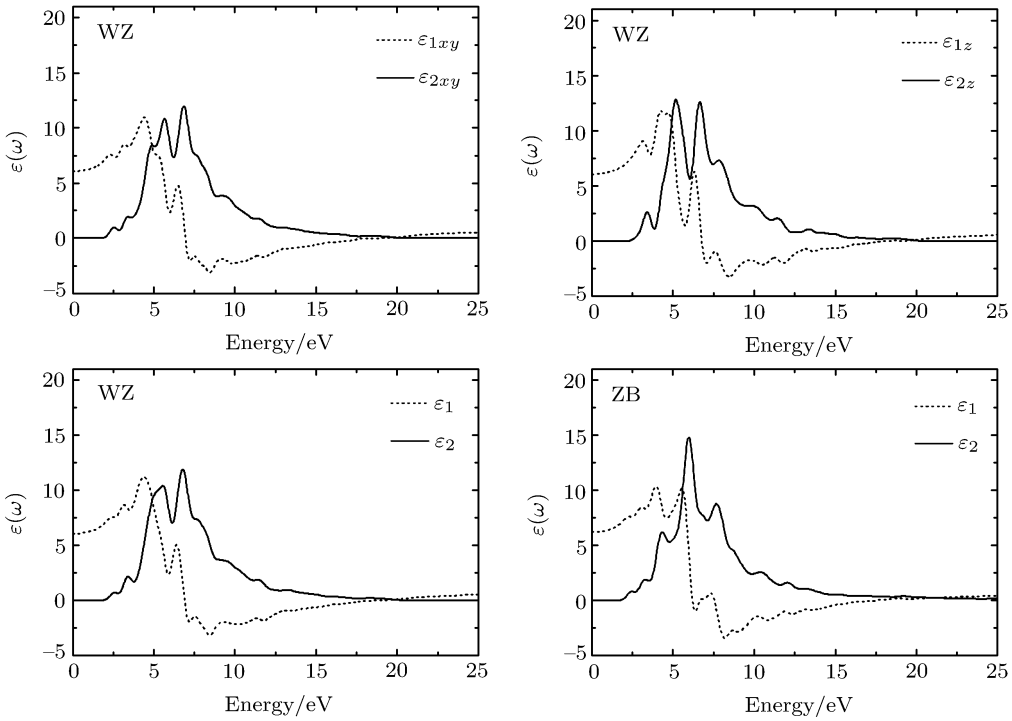


Fig.4. Dielectric functions for the ZB and the WZ structures of ZnS. For ZB-ZnS, $\varepsilon(\omega) = \varepsilon_x(\omega)=\varepsilon_y(\omega)=\varepsilon_z(\omega)$, and for WZ-ZnS, $\varepsilon_x(\omega)=\varepsilon_y(\omega)\neq\varepsilon_z(\omega)$ and $\varepsilon(\omega)=(\varepsilon_x+\varepsilon_y+\varepsilon_z)/3$. The numbers 1 and 2 represent real and imaginary parts of the dielectric function, respectively.

For the real part $\varepsilon_1(\omega)$, the components are similar to those for the imaginary part $\varepsilon_2(\omega)$. From the real part $\varepsilon_1(\omega)$, we can obtain the static electronic dielectric constants $\varepsilon(0)$ easily, which is the value when the energy ($\hbar\omega$) equals zero. So for ZB-ZnS, $\varepsilon(0)=\varepsilon_{1x}(0)=\varepsilon_{1y}(0)=\varepsilon_{1z}(0)$. For the WZ-ZnS, the components of $\varepsilon(0)$ are given by

$$\varepsilon_\perp(0) = (\varepsilon_{1x}(0) + \varepsilon_{1y}(0))/2,$$

and

$$\varepsilon_{//}(0) = \varepsilon_{1z}(0). \quad (3)$$

In this work, $\varepsilon(0)$ for the ZB-ZnS is 6.18, which is smaller than the theoretical value 6.49.[27] The $\varepsilon_\perp(0)$ and $\varepsilon_{//}(0)$ for the WZ-ZnS are 6.06 and 6.08 respectively, which is also a little smaller than the theoretical values 6.71 and 6.90 obtained from empirical calculation.[27] The increased pressure leads to a rapid increase in electronic dielectric constant $\varepsilon(0)$. By fitting the $\varepsilon(0)$–P points to second-order polynomials, we obtain the relationships between $\varepsilon(0)$ and P

ZB:

$$\varepsilon(0) = 6.18 + 1.46\times10^{-4}P + 2.51\times10^{-4}P^2, \quad (4)$$

WZ:

$$\varepsilon_\perp(0) = 6.06 + 2.99\times10^{-3}P + 2.01\times10^{-4}P^2, \quad (5)$$

and

$$\varepsilon_{//}(0) = 6.08 + 7.59\times10^{-3}P + 1.05\times10^{-4}P^2. \quad (6)$$

The electron energy-loss function $L(\omega)$, which is the imaginary part of the reciprocal of the complex dielectric function, is displayed in Fig.5. It is an important factor describing the energy loss of a fast electron traversing in the material. This function is usually

large at the plasmon energy position corresponding to $\varepsilon_1(\omega)$=0, provided that $\varepsilon_2(\omega)$ is reasonably smooth in these regions.[28] Therefore, the ZB-ZnS has a plasmon peak at 18 eV and the WZ-ZnS has a plasmon peak at 19 eV at 0 GPa. With pressure increasing to 27 GPa, the plasmon peak transfers from 18 to 22 eV for the ZB-ZnS, and from 19 to 22 eV for the WZ-ZnS.

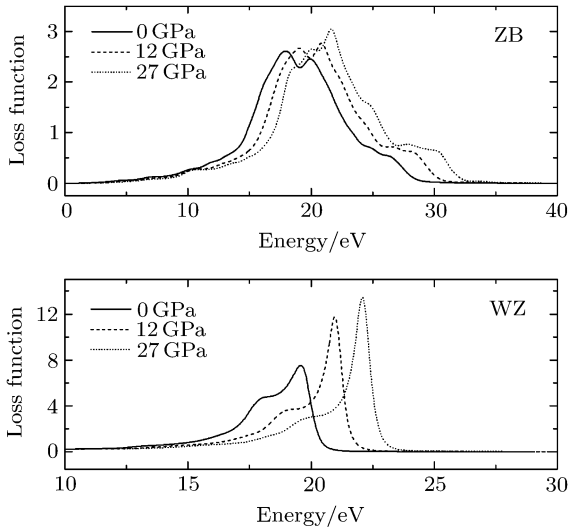


Fig.5. Energy-loss functions for the ZB and the WZ structures of ZnS.

3.3. Thermodynamic properties

The values of Debye temperature Θ and the specific heat capacity C_V at different pressures and different temperatures are presented in Table 2. Using the quasi-harmonic approximation rigid–ion model, Talwar[29] acquired the Debye temperature Θ=370 K for the ZB-ZnS at 0 K and an ambient pressure. And Cline *et al*[30] obtained the Debye temperature Θ=351 K for the WZ-ZnS at 298 K by measuring ultrasonic wave velocities. The heat capacity C_V of the ZB-ZnS 44.27 J·mol^{-1}·K^{-1} at constant volume has been reported by Benkabou *et al*[31] from the molecular dynamics method. Kagayama and Soma[32] obtained the heat capacity C_V of the WZ-ZnS, 44.6 J·mol^{-1}·K^{-1}, from the first-principles calculation at T=300 K and an ambient pressure. Compared with their results under the same condition, our results are satisfactory. The obtained variations in Debye temperature $((\Theta-\Theta_0)/\Theta_0)$ and heat capacity $((C_V-C_{V0})/C_{V0})$ for the two structures of ZnS at various pressures and temperatures are plotted in Figs.6 and 7. It is shown that the values of Debye temperature for two structures ZnS increase with pressure but decrease with temperature. We find a cross point at T=1180 K for the ZB and the WZ structures of ZnS. This is corresponding to the ZB-WZ phase transition temperature 1199 K.[18] On the other hand, the values of heat capacity C_V for two structures decrease with pressure but increase with temperature. At lower temperatures, the value of heat capacity increases quickly, and at higher temperatures, the trend of the increase becomes mild, and close to the Dulong-Petit limit.

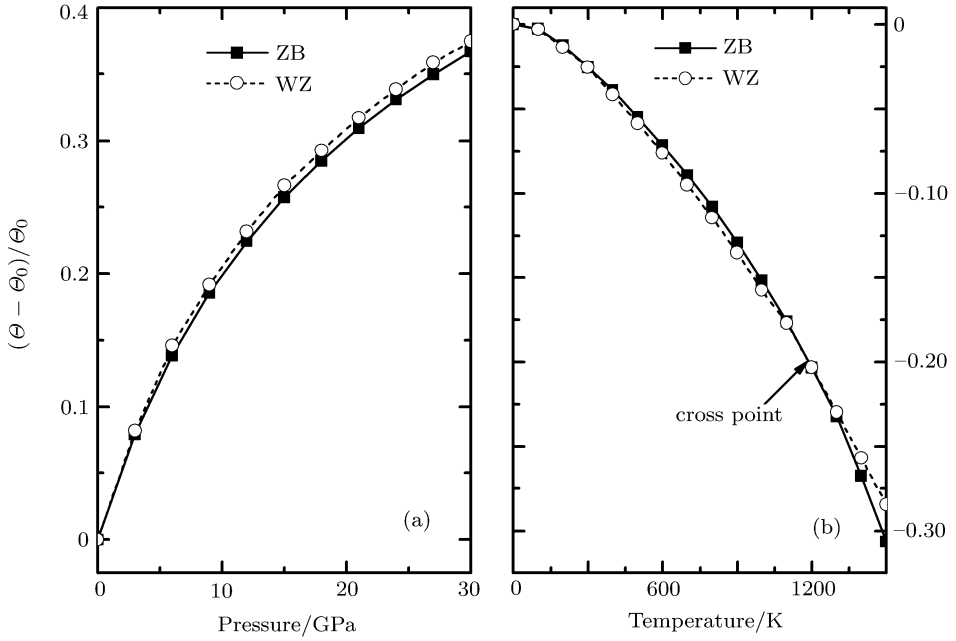


Fig.6. Variations in Debye temperature $(\Theta-\Theta_0)/\Theta_0$ with pressure P under T=0 K (a) and variations of Debye temperature $(\Theta-\Theta_0)/\Theta_0$ with temperature T under P=0 GPa (b), where Θ_0 is the value under zero pressure and zero temperature.

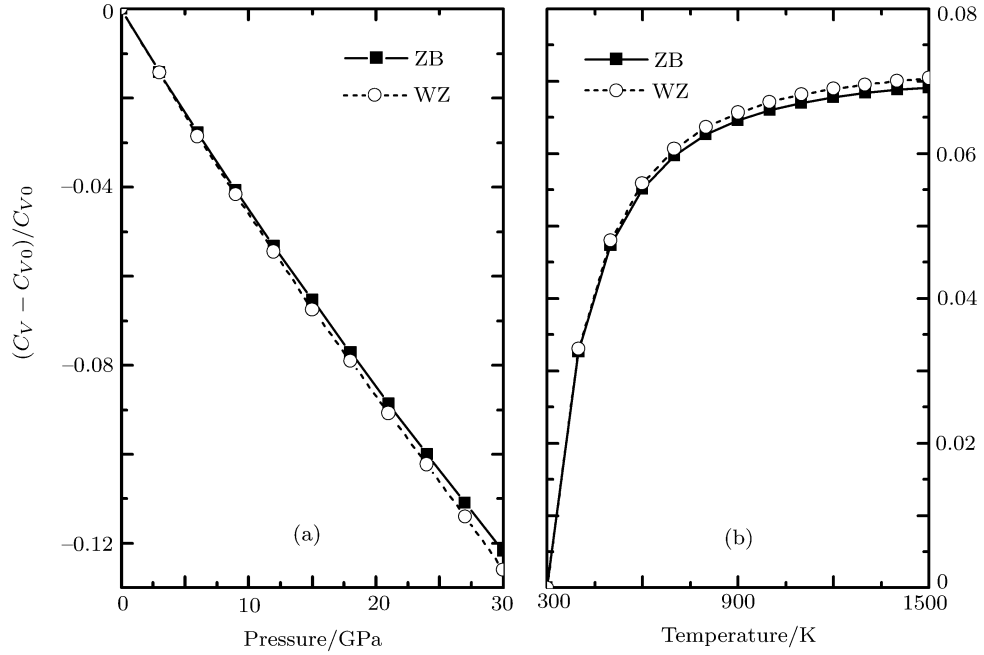


Fig.7. Variations in heat capacity $(C_V - C_{V0})/C_{V0}$ with pressure P under T=300 K (a) and variations of heat capacity $(C_V - C_{V0})/C_{V0}$ with temperature T under P=0 GPa (b), where C_{V0} is the value under 0 GPa and 300 K.

Table 2. The heat capacity C_V (J·mol^{-1}·K^{-1}) and Debye temperature Θ (K) over a wide range of temperatures and pressures.

Pressure/GPa			Temperature/K					
			0	300	600	900	1200	1500
0	ZB	C_V	0	46.29	49.03	49.54	49.71	49.79
		Θ	379.48	370.17	354.17	336.06	315.34	290.45
	WZ	C_V	0	46.35	49.05	49.55	49.718	49.79
		Θ	376.07	366.76	349.42	331.21	312.57	292.79
15	ZB	C_V	0	43.45	48.21	49.16	49.49	49.64
		Θ	510.96	506.34	497.81	488.61	487.97	468.81
	WZ	C_V	0	43.42	48.21	49.16	49.49	49.65
		Θ	512.55	507.58	498.17	488.20	477.95	467.18
30	ZB	C_V	0	41.26	47.55	48.85	49.31	49.53
		Θ	599.44	596.66	590.89	584.29	577.52	570.55
	WZ	C_V	0	41.16	47.53	48.84	49.31	49.53
		Θ	601.30	600.60	593.87	586.64	579.23	571.74

4. Conclusion

We have applied the GGA within the framework of plane-wave pseudopotential DFT method to investigate the electronic, optical and thermodynamic properties of the ZB and the WZ structures of ZnS under pressures. The results obtained are consistent well with other theoretical results and the available experimental data. It is found that the two structures of ZnS have similar direct energy band gaps. When the pressures are above 20.5 and 27 GPa, the ZB-ZnS and the WZ-ZnS are converted into indirect gap semiconductors, respectively. The critical point structure of the frequency dependent complex dielectric function has been investigated and analysed to identify the optical transitions. Moreover, the values of heat capacity C_V and Debye temperature Θ at different pressures and different temperatures are also obtained successfully.

References

[1] Van der Walle C G 1993 *Wide-band-gap Semiconductors* (Amsterdam: North-Holland)

[2] Ma H, Ma G H, Wang W J, Gao X X and Ma H L 2008 *Chin. Phys.* B **17** 1280

[3] Xue L A and Raj R 1990 *J. Mater. Sci. Lett.* **9** 818

[4] Ding Y, Wang X D and Wang Z L 2004 *Chem. Phys. Lett.* **398** 32

[5] Chiang T C, Frank K H, Freund H J, Goldmann A, Himpsel F J, Karlsson U, Leckey R C, Schnieder W D, Koch E E and Bornstein L 1994 *Electronic Structure of Solids: Photoemission Spectra and Related Data, New Series, Group III*, Vol. 23, Part A (Berlin: Springer)

[6] Geng B Y, Liu X W, Du Q B, Wei X W and Zhang L D 2006 *Appl. Phys. Lett.* **88** 163104

[7] Bellotti E, Brennan K F, Wang R and Ruden P R 1997 *J. Appl. Phys.* **82** 2961

[8] Cardona M and Harbeke G 1965 *Phys. Rev.* A **137** 1467

[9] Ebina A, Fukunaga E and Takahashi T 1975 *Phys. Rev.* B **12** 687

[10] Monkhorst H J and Pack J D 1976 *Phys. Rev.* B **13** 5188

[11] Hammer B, Hansen L B and Norskov J K 1999 *Phys. Rev.* B **59** 7413

[12] Perdew J P and Wang Y 1992 *Phys. Rev.* B **45** 13244

[13] Payne M C, Teter M P, Allen D C, Arias T A and Joannopoulos J D 1992 *Rev. Mod. Phys.* **64** 1045

[14] Blanco M A, Francisco E and Luana V 2004 *Comput. Phys. Commun.* **158** 57

[15] Maradudin A A, Montroll E W, Weiss G H and Ipatova I P 1971 *Theory of Lattice Dynamics in the Harmonic Approximation* (New York: Academic Press)

[16] Lu L Y, Chen X R, Yu B R and Gou Q Q 2006 *Chin. Phys.* **15** 802

[17] Hao Y J, Cheng Y, Wang Y J and Chen X R 2007 *Chin. Phys.* **16** 217

[18] Hu C E, Sun L L, Zeng Z Y and Chen X R 2008 *Chin. Phys. Lett.* **25** 675

[19] Ves S, Schwarz U, Christensen N E, Syassen K and Cardona M 1990 *Phys. Rev.* B **42** 9113

[20] Li Q and Wang C 2003 *Appl. Phys. Lett.* **83** 359

[21] Martins J L, Troullier N and Wei S H 1991 *Phys. Rev.* B **43** 2213

[22] Khenata R, Bouhemadou A, Sahnoun M, Reshak A H, Baltache H and Rabah M 2006 *Comput. Mater. Sci.* **38** 29

[23] Rabah M, Abbar B, Al-Douri Y, Bouhafs B and Sahraoui B 2003 *Mater. Sci. Eng.* B **100** 163

[24] Gilbert B, Frazer B H, Zhang H, Huang F, Banfield J F, Haskel D, Lang J C, Srajer G and Stasio G D 2002 *Phys. Rev.* B **66** 245205

[25] Onida G, Reining L and Rubio A 2002 *Rev. Mod. Phys.* **74** 601

[26] Fahy S, Chang K J, Louis S G and Cohen M L 1987 *Phys. Rev.* B **35** 5856

[27] Wright K and Gale J D 2004 *Phys. Rev.* B **70** 035211

[28] Wang C S and Klein B M 1981 *Phys. Rev.* B **24** 3417

[29] Talwar D N 1981 *Phys. Rev.* B **24** 741

[30] Cline C F, Dunegan H L and Henderson G W 1967 *J. Appl. Phys.* **38** 1944

[31] Benkabou F, Aourag H and Certier M 2000 *Mater. Chem. Phys.* **66** 10

[32] Kagayama H M and Soma T 1986 *Phys. Status Solidi* B **134** 101